Published December 3, 2015

RESEARCH

Extending the Marker × Environment Interaction Model for Genomic-Enabled Prediction and Genome-Wide Association Analysis in Durum Wheat

José Crossa,* Gustavo de los Campos, Marco Maccaferri, Roberto Tuberosa, J. Burgueño, and Paulino Pérez-Rodríguez*

ABSTRACT

The marker × environment interaction (M×E) genomic model can be used to generate predictions for untested individuals and identify genomic regions in which effects are stable across environments and others that show environmental specificity. The objectives of this study were (i) to extend the M×E model using priors that produce shrinkage and variable selection such as Bayesian ridge regression (BRR) and BayesB (BB), respectively, and (ii) to evaluate the genomic prediction accuracy of M×E, single-environment, and across-environment models using a multiparental durum wheat (*Triticum turgidum* L. spp. *duram*) population characterized for grain yield (GY), grain volume weight (GVW), 1000-kernel weight (GWT), and heading date (HD) in four environments. Breeding value predictions were generated for two prediction problems: cross-validation problem 1 (CV1) and cross-validation problem 2 (CV2). In general, results showed that the M×E model performed better than the single-environment and across-environment models, in terms of minimizing the model residual variance, for both CV1 and CV2. The improved data-fitting gain over the other models was more evident for GWT and HD (up to twofold differences) than to GY and GVW, which showed more complex genetic bases and smaller single-marker effects. Considering the Bayesian models used, BB showed better overall prediction accuracy than BRR. As proof-of-concept for the M×E model, the major controllers of HD—*Ppd* and *FT* on chromosomes 2A, 2B, and 7A—showed stable effects across environments as well as environment-specific effects. For GY, besides the regions on chromosomes 2B and 7A, additional chromosome regions with large marker effects were detected in all chromosome groups.

J. Crossa and J. Burgueño, Biometrics and Statistics Unit, International Maize and Wheat Improvement Center (CIMMYT), Apdo. Postal 6-641, Mexico DF, 06600 Mexico; G. de los Campos, Epidemiology & Biostatistics and Statistics Deps., Michigan State Univ., 909 Fee Rd., East Lansing, MI 48824; R. Tuberosa and M. Maccaferri, Dep. of Agricultural Sciences, Univ. of Bologna, Viale Fanin 44, 40127, Bologna, Italy; P. Pérez-Rodríguez, Colegio de Postgraduados, Statistics and Computer Sciences, Montecillos, Edo. de Mexico, Mexico. Received 22 Apr. 2015. Accepted 28 July 2015. *Corresponding authors (perpdgo@gmail.com; j.crossa@cgiar.org).

Abbreviations: aBB, across-environment BayesB**;** aBRR, across-environment Bayesian ridge regression; BB, BayesB; BRR, Bayesian ridge regression; CV1, cross-validation problem 1; CV2, cross-validation problem 2; GBLUP, genomic best linear unbiased prediction; GS, genomic selection; GVW, grain volume weight; GWT, 1000-kernel weight; GY, grain yield; G×E, genetic × environment interaction; HD, heading date; M×E, marker × environment interaction; NCCR, 'Neodur', 'Claudio', 'Colosseo', and 'Rascon/Tarro'; QTL, quantitative trait loci; RIL, recombinant inbred line; sBB, single-environment BayesB; sBRR, single-environment Bayesian ridge regression; SNP, single-nucleotide polymorphism; TRN-TST, training–testing; TRN, training; TST, testing.

Genetic × environment interaction (G×E) affects trait heritability and the relative rankings of phenotypes across environments; this introduces challenges when making breeding decisions. The effects of G×E on heritability may be due to scale effects such as changes in the size of quantitative trait loci (QTL) effects across environments or to differential genetic effects on environmental variance. However, G×E can also modulate QTL effects, thus introducing changes in the relative rank of genotypes across environments (Dickerson, 1962; Cockerham, 1963). Falconer (1952) suggested modeling performance in two environments as two correlated traits; this allows modeling both scale effects and rerankings.

Published in Crop Sci. 56:2193–2209 (2016).
doi: 10.2135/cropsci2015.04.0260

Knowledge of the genetic basis of adaptation and its physiological and environmental causes is essential for understanding G×E, for interpreting the causal association between phenotype and genotypes at particular loci, and for enhancing the selection of superior and stable genotypes. This issue is particularly relevant when considering highly contrasting environments and QTL performance (Collins et al., 2008; Maccaferri et al., 2008; Bennett et al., 2012; Bonneau et al., 2013; Heslot et al., 2014). A shortcoming of many of the statistical multienvironment models commonly used in plant breeding is that they deal with G×E implicitly, without explicitly modeling gene (marker) × environment interactions. Such an approach does not shed light on the underlying genetic architecture of G×E. Examples of methods that deal with G×E implicitly without modeling M×E include the family of linear-by-linear models of Cornelius et al. (1996) as well as more modern methods such as the multivariate pedigree- or marker-based models, where G×E is modeled using structured or unstructured covariance functions (e.g., Piepho, 1997, 1998; Smith et al., 2005; Crossa et al., 2006; Burgueño et al., 2007, 2012; El-Soda et al., 2014). When genomic data are available, G×E can be modeled explicitly by means of M×E when marker effects can vary among environments or groups of environments and by recognizing that these effects may be correlated. This approach was first used with sparse marker data in QTL analysis (Moreau et al., 2004) and, in many cases, was based on a limited number of markers (Boer et al., 2007).

Genomic-enabled prediction models for genomic selection (GS) using all available markers were originally presented by Meuwissen et al. (2001). After this original study, several genomic prediction models were developed and applied in simulated and real plant breeding data (e.g., Bernardo and Yu, 2007; de los Campos et al., 2009, 2013; Crossa et al., 2010; Pérez-Rodríguez et al., 2012). In general, these studies showed good prediction accuracies for GY and other traits evaluated by means of several random cross-validation partitions of the data. The first public study confirming these previous findings on genomic-enabled prediction was that of Massman et al. (2013), who showed that genomic selection improved genetic gains per unit of time in one biparental temperate maize (*Zea mays* L.) population. Recently, Beyene et al. (2015) achieved important genetic gains in GY through genomic selection in eight tropical biparental CIMMYT maize populations; these authors evaluated cycles of genomic selection in severe drought environments in sub-Saharan Africa. These results have prompted other CIMMYT maize and bread wheat breeding programs to quickly adopt GS.

Originally, genomic-enabled prediction models and methods were developed and used without considering G×E. Burgueño et al. (2012) extended the GS model to accommodate G×E in a genomic best linear unbiased prediction (GBLUP) context. More recently, Heslot et al. (2014) and Jarquín et al. (2014) proposed GS models that incorporate both markers and environmental covariates in the G×E model, while López-Cruz et al. (2015) considered a GS model that incorporates M×E. These studies have demonstrated that incorporating G×E can lead to substantial increases in prediction accuracy relative to either within-environment analyses or an across-environment analysis that ignores G×E.

The M×E GS model presented by López-Cruz et al. (2015) can be employed not only for genomic-enabled prediction but also for identifying genomic regions in which the effects are stable across environments and other regions that are specific to certain environments and therefore responsible for G×E. Results of the M×E model proposed by López-Cruz et al. (2015) on three extensive bread wheat data sets showed that (i) the proportion of genomic variance explained by the main effect is a good estimator of the phenotypic correlation between environments, and (ii) depending on the validation problem and on the correlation between environments, the M×E model can yield important gains in prediction accuracy over the single-environment and across-environment models. However, López-Cruz et al. (2015) did not use the M×E model for identifying chromosomic regions in genome-wide association analyses.

Standard multienvironment mixed-model approaches (e.g., Piepho, 1997, 1998; Smith et al., 2005; Crossa et al., 2006; Burgueño et al., 2007, 2012) rely on Gaussian assumptions; when applied to genomic data, these approaches induce shrinkage (i.e., reduce marker effects) but not variable (marker) selection. One advantage of the M×E model is that it can be used with prior information that induces shrinkage as well as priors that produce variable selection. The application presented by López-Cruz et al. (2015) is based on a shrinkage method (a ridge-regression type estimator). Here, we extend this approach to variable selection methods by means of the BB model, although the methodology can be extended also to include other members of the Bayesian alphabet (Gianola, 2013).

In durum wheat, Abdalla et al. (1997) and Trethowan et al. (2005) pointed out that targeted genetic progress could be achieved by subdividing global durum areas into more homogenous subregions, thus reducing G×E. Recent studies in durum wheat included extensive association mapping for agronomic traits for a reference population evaluated under different water regimes (Maccaferri et al., 2011) and a high-density single-nucleotide polymorphism (SNP) map (Maccaferri et al., 2014; Milner et al., 2015). Although in recent years genomic prediction has been applied to bread wheat (de los Campos et al., 2009, 2010; Crossa et al., 2010; González-Camacho et al., 2012; Heslot et al., 2012; Pérez-Rodríguez et al., 2012; López-Cruz et al., 2015), to our best knowledge, no study

has been reported on (i) genomic prediction accuracy of traits measured in durum wheat, and (ii) the use of the M×E model with variable selection and with marker main effect and environment marker-specific effects.

The main objectives of this study were (i) to extend and demonstrate the use of the M×E model of López-Cruz et al. (2015) but using priors that induce shrinkage (BRR) as well as variable selection (BB) and (ii) to evaluate these GS models using a durum wheat population comprising a balanced, four-parental cross (identified as NCCR) (Milner et al., 2015) evaluated for HD, GVW, GWT, and GY in four environments. One problem we assessed was how to generate breeding-value predictions for additional lines for which phenotypic data were not available (cross-validation problem 1, or CV1); another problem was how to predict breeding values for lines observed in some environments but not in others (cross-validation problem 2, or CV2). We also show how the M×E model, when implemented with priors that induce variable selection, can provide information on which genomic regions contribute the most to stability and to interaction effects. Furthermore, we applied the M×E model considering heterogeneity of within-environment error variance as an extension of the López-Cruz et al. (2015) model that was originally used assuming homogeneity of within-environment error variance.

MATERIALS AND METHODS

Genotypic and Phenotypic Data

Details of phenotypic and genotypic data as well as how the multiparental population was developed are given in Milner et al. (2015); a brief description is given below.

Development of the Multiparental NCCR Population

A balanced, four-way multiparental cross population was developed from four elite durum wheat cultivars (Neodur, Claudio, Colosseo, and Rascon/Tarro) that were chosen as diverse contributors of different alleles of agronomic relevance. The cultivars were crossed pair-wise following the scheme ([Neodur × Claudio] × [Colosseo × Rascon/Tarro], i.e., NCCR) to produce two-way F_1 hybrids that were subsequently crossed to produce 400 four-way F_1 NCCR hybrids. These four-way F_1 hybrids were advanced through single-seed descent and bulked in the F_8 generation. The final NCCR population includes 338 recombinant inbred lines (RILs) (Milner et al., 2015). This population is representative of segregating populations commonly used in wheat breeding, where the three- and four-way cross scheme is increasingly adopted to generate wider genotypic variance in segregating populations as compared with the traditional biparental cross. Importantly, the balanced NCCR population shows almost no population structure (Milner et al., 2015), making it a much more suitable material for assessing the performance of M×E models than collections of diverse cultivars and breeding lines commonly used in association mapping studies.

Genotypic Data

The final number of SNPs included in the NCCR linkage map was 7594. The markers were centered and standardized before being used in the GS models. The NCCR linkage map was estimated using the program mpMap (Huang and George, 2011), an R package specifically written for analyzing multiparental populations. Maximum likelihood estimates of the recombination fraction (r) between each SNP pair were obtained using the *mpestrf* function with default parameter settings.

Phenotypic Data

Phenotypic evaluation of the NCCR population was performed during two growing seasons (2010–2011 and 2011–2012) in locations in the Po Valley representative of the target environments where durum wheat is grown: Cadriano (44°33′ N 11° 26′ E) in the 2010–2011 growing season (Cad11) and the 2011–2012 growing season (Cad12); Poggio Renatico (44°46′ N 11°30′ E) in the 2010–2011 growing season (Pr11), and Argelato (44°34′ N 11°20′ E) in the 2011–2012 growing season (Arg12). The 338 RILs, the four parents, and the five control genotypes were evaluated in an α-lattice incomplete-block experimental design; a 19 by 19 α-lattice design with two replications was considered in each environment. The genotype least squares means were adjusted for a lattice, with incomplete blocks considered as random effects to recover interblock information.

The four traits included in this study were GY (Mg ha^{-1}), HD (d), GWT (g 1000 kernels^{-1}), and GVW (kg hL^{-1}). The phenotypes of the four traits used for data analysis were the best linear unbiased estimates after recovering the incomplete block information (i.e., adjusting for the random incomplete block effect) in each environment and across environments.

Statistical Models

The M×E model extends the approach described in López-Cruz et al. (2015) by incorporating priors that can induce variable selection and allowing for environment-specific error variances. We performed a combined analysis based on an M×E model from which within-environment analysis (also referred to as single-environment model or stratified analysis) and across-environment analysis can be derived and computed.

Marker × Environment Interaction Regression Model

In an interaction model, the effect of the kth marker in the jth environment is modeled as the sum of a main effect (b_{0k}) plus an interaction term b_{jk} representing deviations from the main effect resulting from M×E. Thus, the marker effect model for the kth marker in the jth environment is $\beta_{jk} = b_{0k} + b_{jk}$. With this, the regression equation for the ith line in the jth environment, y_{ij}, becomes

$$y_{ij} = \mu_j + \sum_{k=1}^{p} x_{ijk}\left(b_{0k} + b_{jk}\right) + \varepsilon_{ij}$$

or, in matrix notation and assuming s environments,

$$\begin{bmatrix}\mathbf{y}_1\\ \vdots\\ \mathbf{y}_s\end{bmatrix}=\begin{bmatrix}1\boldsymbol{\mu}_1\\ \vdots\\ 1\boldsymbol{\mu}_s\end{bmatrix}+\begin{bmatrix}\mathbf{X}_1\\ \vdots\\ \mathbf{X}_s\end{bmatrix}\mathbf{b}_0+\begin{bmatrix}\mathbf{X}_1 & \mathbf{0} & \cdots & \mathbf{0}\\ \mathbf{0} & \mathbf{X}_2 & \cdots & \mathbf{0}\\ \vdots & \vdots & \ddots & \mathbf{0}\\ \mathbf{0} & \mathbf{0} & \cdots & \mathbf{X}_s\end{bmatrix}\begin{bmatrix}\mathbf{b}_1\\ \vdots\\ \mathbf{b}_s\end{bmatrix}+\begin{bmatrix}\boldsymbol{\varepsilon}_1\\ \vdots\\ \boldsymbol{\varepsilon}_s\end{bmatrix} \quad [1]$$

where $\boldsymbol{\mu}=\begin{bmatrix}1\boldsymbol{\mu}_1\\ \vdots\\ 1\boldsymbol{\mu}_s\end{bmatrix}$ is a vector of intercepts and $\mathbf{X}=\begin{bmatrix}\mathbf{X}_1\\ \vdots\\ \mathbf{X}_s\end{bmatrix}$ is a matrix of marker-centered and standardized genotypes for each of the s environments. In the ridge regression BLUP or GBLUP context, the vectors of main marker effects, M×E effects, and residual effects are all assumed to be normally distributed, $\mathbf{b}_0 \sim N\left(\mathbf{0},\mathbf{I}\sigma^2_{b_0}\right)$, $\mathbf{b}_j \sim N\left(\mathbf{0},\mathbf{I}\sigma^2_{b_j}\right)$, and $\boldsymbol{\varepsilon}_j \sim N\left(\mathbf{0},\mathbf{I}\sigma^2_{\varepsilon}\right)$, respectively. The model in Eq. [1] is described as an M×E ridge regression BLUP (or M×E GBLUP model).

López-Cruz et al. (2015) assume homoscedasticity of environmental residuals (i.e., equal variance for all the environments), that is, $\boldsymbol{\varepsilon} \sim N\left(\mathbf{0},\mathbf{I}\sigma^2_{\varepsilon}\right)$. In this study, we relax this assumption and use the heterogeneity of residual environmental variances, such that $\boldsymbol{\varepsilon} \sim N\left(\mathbf{0},\mathbf{D}\otimes\mathbf{I}_n\right)$, where $\mathbf{D}$ = diag $(\sigma^2_{\varepsilon_1},\sigma^2_{\varepsilon_2},\ldots,\sigma^2_{\varepsilon_s})$ with $\sigma^2_{\varepsilon_1},\ldots,\sigma^2_{\varepsilon_s}$ denoting the residual variance for environments 1,...,s, respectively, and $\mathbf{I}_n$ is an n-dimensional identity matrix.

Single-Environment Regression and Across-Environment Regression Models

A single-environment (or within-environment) regression model can be obtained as a special case of the model in Eq. [1] by removing the main effects of markers, $\mathbf{b}_0 = \mathbf{0}$, such that

$$\begin{bmatrix}\mathbf{y}_1\\ \vdots\\ \mathbf{y}_s\end{bmatrix}=\begin{bmatrix}1\boldsymbol{\mu}_1\\ \vdots\\ 1\boldsymbol{\mu}_s\end{bmatrix}+\begin{bmatrix}\mathbf{X}_1 & \mathbf{0} & \cdots & \mathbf{0}\\ \mathbf{0} & \mathbf{X}_2 & \cdots & \mathbf{0}\\ \vdots & \vdots & \ddots & \mathbf{0}\\ \mathbf{0} & \mathbf{0} & \cdots & \mathbf{X}_s\end{bmatrix}\begin{bmatrix}\mathbf{b}_1\\ \vdots\\ \mathbf{b}_s\end{bmatrix}+\begin{bmatrix}\boldsymbol{\varepsilon}_1\\ \vdots\\ \boldsymbol{\varepsilon}_s\end{bmatrix} \quad [2]$$

This is equivalent to regressing phenotypes on markers in each environment, that is, fitting a GS model. Alternatively, a special case of Eq. [2] is the across-environment regression model that assumes constant marker effects across the environments, $\mathbf{b}_1 = \mathbf{b}_2 = \cdots = \mathbf{b}_s = \mathbf{b}$, such that,

$$\begin{bmatrix}\mathbf{y}_1\\ \vdots\\ \mathbf{y}_s\end{bmatrix}=\begin{bmatrix}1\boldsymbol{\mu}_1\\ \vdots\\ 1\boldsymbol{\mu}_s\end{bmatrix}+\begin{bmatrix}\mathbf{X}_1\\ \vdots\\ \mathbf{X}_s\end{bmatrix}\mathbf{b}+\begin{bmatrix}\boldsymbol{\varepsilon}_1\\ \vdots\\ \boldsymbol{\varepsilon}_1\end{bmatrix} \quad [3]$$

Models [1] to [3] were fitted by using Bayesian estimation methods. Next, we describe the prior distributions.

Prior Distributions

The intercepts were assigned flat priors, the error variances were assigned weakly informative, scaled, inverse Chi squared densities with five degrees of freedom, and the scale parameter was estimated from marker data for each dataset; for further details see Pérez-Rodríguez and de los Campos (2014) (see section B: Default Rules for Choosing Hyper-Parameters for Variance Parameters). Marker effects were assigned either Gaussian priors (BRR, equivalent to the GBLUP model) or a two-component mixture with a point of mass at zero and a t-slab (the so-called BB BayesB model, Meuwissen et al., 2001). The Gaussian prior induces shrinkage of estimates of effects; on the other hand, the mixture prior used in model BB can induce variable selection and shrinkage simultaneously. The variance of the marker effects in BRR, the proportion of nonnull effects in BB, and the scale of the t-slab were estimated from data, as implemented in the BGLR software (de los Campos and Pérez–Rodríguez, 2014).

Full Data Analyses

The models described above were first fitted to the full data set on a trait-by-trait basis. Analyses using the full data had two aims: (i) to derive estimates of variance components and (ii) to estimate markers effects for the genome-wide association analyses. Full data were used to estimate the posterior variance components resulting from residual effects, marker main effect, and environment-specific effects from the single-environment BRR (sBRR) model, the M×E BRR model, and the across-environment BRR (aBRR) model for the four traits measured in four environments.

It should be pointed out that the information generated from the full data analyses was not used as prior information for the random cross-validation partition schemes (CV1 and CV2) employed for assessing the prediction accuracy of the different models.

Random Cross-Validations Partitions of the Data for Assessing Prediction Accuracy

Prediction accuracy was assessed using replicated training–testing (TRN-TST). Within each TRN-TST partition, a set of lines comprising 80% of the records were selected and used as training models (TRN, 270 durum wheat lines); the remaining 20% of the records (TST, 68 durum wheat lines) were used to assess prediction accuracy. For each of the 50 partitions, all the posterior variance components resulting from residual effects, marker main effect, environment-specific effects from the single-environment, the M×E, and the across-environment BRR models for the four traits were re-estimated.

The pattern of missing values was generated using a cross-validation scheme that mimics two prediction problems commonly encountered in plant breeding (Burgueño et al., 2012). The first prediction problem in cross-validation (CV1) predicts 20% of the unobserved durum wheat lines that were not evaluated in any of the four environments (validation set, TST); this CV1 mimics the situation were newly developed durum wheat lines that have never been observed in any of the environments must be predicted (in each of those environments). For CV1, the TRN and TST populations were randomly assigned: 80% to TRN and 20% to TST. The second prediction problem in cross-validation (CV2) assumes that 20% of the durum wheat lines were evaluated in some environments but not in others. The CV2 prediction problem is similar to the one plant breeders face when using a sparse field design evaluation

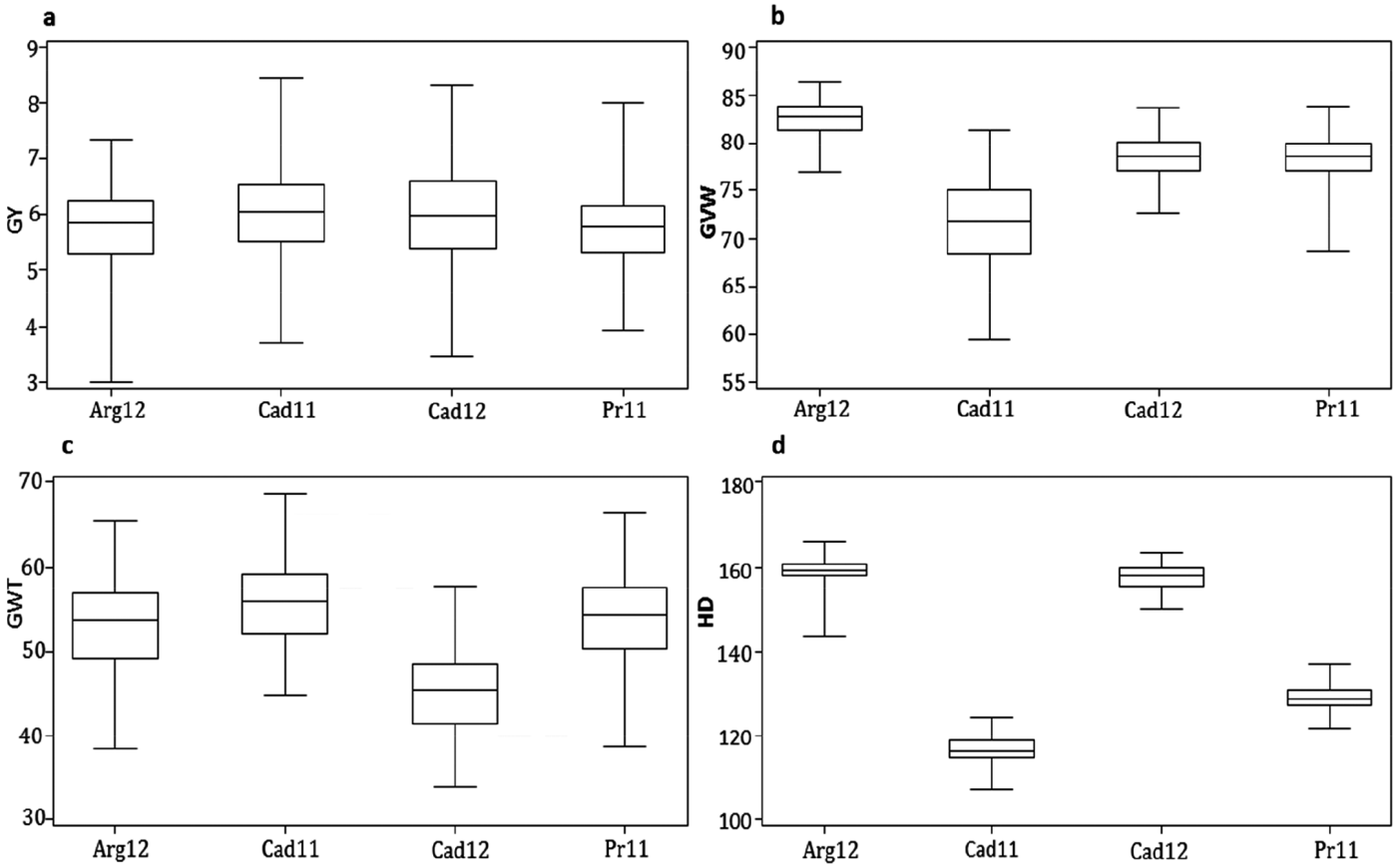

Figure 1. Box plot of adjusted means for (a) grain yield (GY, Mg ha^{-1}), (b) grain volume weight (GVW, kg hL^{-1}), (c) 1000-kernel weight (GWT, g 1000 kernels^{-1}), and (d) days to heading (HD, d) in four environments (Arg12, Cad11, Cad12, and Pr11).

where some lines are evaluated in some environments but not in others. In CV2, some durum wheat lines are predicted in environments that were not phenotypically evaluated.

We used 50 random partitions of the TRN-TST design described above; for each TRN-TST design, models were fitted to the training data set and prediction accuracy was assessed by computing Pearson's product–moment correlation between predictions and observed phenotypes in the testing data set within environments and across environments. Thus, 50 correlations were computed for each model and trait, and the mean and standard deviations of these 50 correlations are reported.

Software

The models described above were implemented using the R package (R Development Core Team, 2014) Bayesian Generalized Linear Regression (BGLR; de los Campos and Pérez-Rodríguez, 2015), release 1.0.4, available at CRAN, http://cran.r-project.org/web/packages/BGLR/index.html, which supports heterogeneous variances in the model residuals.

RESULTS

Statistics Descriptive of the Data

Box plots of traits GY, GVW, GWT, and HD in each of the environments are depicted in Fig. 1. For GY, the four environments showed similar potential (average GY ranging between 5.5 and 6.0 Mg ha^{-1}; Fig. 1a); however, for HD, environments Arg12 and Cad12 were much later than environments Cad11 and Prn11 (Fig. 1d). Sample phenotypic correlations among the four environments for the four traits are given in Table 1. Most of the pair-wise environments had a positive and, in some cases, high correlation, especially for HD and GWT. The exceptions were those cases where the correlation of environments was equal or very close to zero, for example, GY for environment pairs Cad12-Cad11 (0.0578), Cad12-Arg12 (0.1708), and Pr11-Cad12 (0.0246), and GVW for environment pairs Cad11-Arg12 (0.0188), Cad11-Cad12 (−0.0190), Pr11-Cad11 (−0.0540), and Pr11-Cad12 (0.1626). In all environments, GY and GVW had markedly lower heritability (from 0.2578 to 0.3413 and from 0.2146 to 0.4684, respectively) than GWT and HD (from 0.5672 to 0.6575).

Variance Component Estimates

Estimates of residual and genomic variance components for the single-environment, M×E, and across-environment models (derived from BRR and BB and the different traits and environments) are based on full data analyses and presented in the following sections. Marker main effects and environment marker-specific effects are also based on full data analyses.

Table 1. Phenotypic correlations among four environments (Arg12, Cad11, Cad12, and Pr11) for grain yield (GY), grain volume weight (GVW), 1000-kernel weight (GWT), and days to heading (HD). Heritability (H^2) of the four traits in each of the four environments (standard deviation in parentheses).

	Lower diagonal GY, upper diagonal GVW			
Environment	Arg12	Cad11	Cad12	Pr11
Arg12	–	0.0188	0.3422	0.1128
Cad11	0.3420	–	−0.0190	−0.0540
Cad12	0.1708	0.0578	–	0.1626
Pr11	0.3009	0.4748	0.0246	–
	Lower diagonal GWT, upper diagonal HD			
Arg12	–	0.7744	0.7702	0.7851
Cad11	0.8513	–	0.8302	0.9272
Cad12	0.8003	0.7608	–	0.8109
Pr11	0.8795	0.8603	0.7596	–
	Heritability			
	GY	GVW	GWT	HD
Arg12	0.3413 (0.0636)	0.3262 (0.0651)	0.6575 (0.0551)	0.4696 (0.0713)
Cad11	0.2820 (0.0548)	0.2146 (0.0453)	0.6143 (0.0589)	0.6700 (0.0654)
Cad12	0.2578 (0.0530)	0.4684 (0.0744)	0.5672 (0.0629)	0.6038 (0.0676)
Prn11	0.3253 (0.0647)	0.2218 (0.0455)	0.6384 (0.0572)	0.5890 (0.0714)

Residual Variances

Estimates (estimated posterior means) of the residual variance parameters from the M×E, single-environment (sBRR, sBB) and across-environment (aBRR, aBB) models derived from BRR and BB are given in Table 2 and Table 3, respectively; general patterns and trends are depicted in Fig. 2 for model BRR and Fig. 3 for model BB for the four traits in each environment. For all traits and environments, the estimated residual variances for the M×E model derived from the BRR and BB models were always smaller than those derived from the single-environment and across-environment BRR and BB models. These results indicate the M×E model derived from BRR or BB fits the data better than models that (i) force the marker effects to be constant across environments and (ii) single-environment models. The patterns of residual variance for the single-environment, M×E, and across-environment models derived from BRR and BB are very similar and do not indicate that overall BRR gives a better fit than BB, or vice versa. For all models and environments, residual variances are much smaller for the simpler traits GWT and HD than for the more complex (and less heritable) traits such as GY and GVW.

Genomic Variances

In the genomic variance components derived from BRR, the single-environment model estimates separate marker variances for each environment, whereas, in the BRR across environments, just one marker variance (the same for all environments) is estimated. In the M×E BRR interaction model, a marker main effect and a marker-specific effect for each environment are estimated. In the M×E BB interaction model, marker effects are given in terms of the probability or proportion of markers with effects different from zero (nonnull) that are estimated for each of the components of the marker effects (i.e., main effect and environment marker specific effect) (see Table 2 for BRR and Table 3 for BB).

As previously mentioned, in the M×E BRR interaction model, the total genomic variance is portioned into the marker main effects and the environmental marker-specific effect. Figure 4 depicts the percentages of the main and specific marker effects for each trait and environment. For GY, the marker main effects explained ~55 to 62% of the total genomic variance in all environments, whereas the specific marker variance in each environment was ~38 to 45% (Fig. 4a). For GVW, the marker main effect explained ~30 to 41%, whereas the markers that had specific variance effects in each environment accounted for 59 to 70% (Fig. 4b). For less complex traits (GWT and HD), the marker main effect explained most of the total genomic variance (>90%) with a small marker environmental specific variance for all environments (Figs. 4c, d). Note that the marker variance component of the main effect for HD was 2.3388 with a SD 0.1649 (Table 2 for BRR), indicating the uncertainty of this variance component estimate. This is likely due to the great variance of HD among the four environments (see the box plot in Fig. 1d), which inflates $\sigma^2_{b_0}$.

The estimated proportion of markers with nonnull effects given by the BB model varies depending on the trait and the model. Overall, the across-environments BB model (aBB) had a lower proportion of markers with nonnull effect than the M×E BB model (Table 3), and fewer nonnull markers were found for trait HD than GY and GVW. For example, model aBB gave proportions of 13.34, 28.57, 34.82, and 39.35% of markers with nonnull effects for HD, GWT, GVW, and GY, respectively,

Table 2. Estimated posterior variance components as a result of residual, marker main effect, and environment-specific effects (and their posterior standard deviations, SD) from the single-environment Bayesian ridge regression model (sBRR), the marker × environment interaction Bayesian ridge regression model (M×E BRR), and the across-environment Bayesian ridge regression model (aBRR) for grain yield (GY), grain volume weight (GVW), 1000-kernel weight (GWT), and days to heading (HD) measured in four environments (Arg12, Cad11, Cad12, and Pr11).

		GY		GVW		GWT		HD	
	Environment	Estimate	SD	Estimate	SD	Estimate	SD	Estimate	SD
		Single-environment Bayesian ridge regression (sBRR)							
Residual	Arg12	0.7133	0.0743	0.7343	0.0766	0.3124	0.0393	0.5670	0.0664
	Cad11	0.7708	0.0733	0.8623	0.0769	0.3461	0.0419	0.3903	0.0582
	Cad12	0.8036	0.0763	0.5754	0.0689	0.4132	0.0491	0.4434	0.0589
	Pr11	0.7384	0.0770	0.8439	0.0764	0.3368	0.0417	0.4636	0.0624
Marker	Arg12	0.3722	0.0841	0.3582	0.0852	0.6088	0.1007	0.5089	0.109
	Cad11	0.3042	0.0686	0.2363	0.0554	0.5595	0.0974	0.8091	0.148
	Cad12	0.2804	0.0657	0.5146	0.1147	0.5495	0.1018	0.6880	0.1326
	Pr11	0.3585	0.0850	0.2410	0.0549	0.6038	0.1027	0.6770	0.1362
		M × E interaction Bayesian ridge regression (M×E BRR)							
Residual	Arg12	0.6403	0.0629	0.7123	0.0688	0.1195	0.0132	0.2312	0.0237
	Cad11	0.6624	0.0666	0.8468	0.0815	0.1561	0.0185	0.0918	0.0116
	Cad12	0.7738	0.0771	0.5796	0.0668	0.2406	0.0254	0.1686	0.0190
	Pr11	0.6400	0.0646	0.8166	0.0720	0.1456	0.0165	0.1050	0.0126
Marker environment main effect and specific effect	Main effect	0.2853	0.0753	0.1273	0.0457	1.4130	0.1564	2.3388	0.1649
	Arg12	0.1780	0.0471	0.1820	0.0511	0.0703	0.0127	0.0881	0.0182
	Cad11	0.1963	0.0459	0.2635	0.0716	0.1064	0.0200	0.0803	0.0135
	Cad12	0.2422	0.0727	0.2936	0.1046	0.1133	0.0280	0.1096	0.0261
	Pr11	0.2071	0.0704	0.2008	0.0635	0.0931	0.0211	0.0814	0.0173
		Across-environment Bayesian ridge regression (aBRR)							
Residual	Arg12	0.7517	0.0660	0.7827	0.0674	0.1392	0.0138	0.2725	0.0244
	Cad11	0.7404	0.0643	1.0626	0.0882	0.2063	0.0197	0.1148	0.0130
	Cad12	1.0012	0.0874	0.7347	0.0670	0.3080	0.0269	0.2471	0.0227
	Pr11	0.7127	0.0634	0.9082	0.0732	0.1757	0.0171	0.1236	0.0127
Marker	Main effect	0.3123	0.0590	0.1918	0.0380	1.3635	0.1193	2.3045	0.2408

whereas the M×E BB model gave, for the marker main effect, proportions of 40.74, 48.50, 53.12, and 51.15% of markers with nonnull effect for traits HD, GWT, GVW, and GY, respectively.

Marker Main Effects and Environment-Specific Effects

The M×E BB model induces variable (marker) selection and thus offers the possibility of examining the response patterns of the marker main effects and environment-specific marker effects. For trait HD, the marker main effect showed specific regions of chromosomes 2A, 2B, and 7A, with large marker main effects (Fig. 5a). Based on the gene-tagging SNPs used to construct the map and perform the synteny analysis, these regions correspond to main effects at candidates *PPD-A1*, *PPD-B1* and *TaFTA*, respectively (Milner et al., 2015). For environment-specific marker effects, the M×E BB model evidenced one marker in chromosome 2A that had a prominent role in environment Cad11 (Fig. 5b). Chromosome position (in cM), absolute value of the marker effects in days for trait HD for the marker main effect and specific environmental effect for the markers with the highest effects outlined in Fig. 5 are given in Supplemental Table S1 (see http://hdl.handle.net/11529/10233).

For GY (a complex trait), the patterns of marker main effects and environment-specific effects are not as clearly depicted as those for HD (a much less complex trait). The marker main effect detected by the M×E BB model evidenced important regions of chromosomes 2A, 2B, 3A, 5A, 5B, and 7A (Fig. 6a); these regions are also related to *PPD-B1* and *TaFTA* effects as well as to the regions of chromosomes 3A, 5A, and 5B. Markers with environment-specific effects were found on chromosomes 1B, 4B, and 7A in Arg12 (Fig. 6b), on chromosomes 2A, 3A, 5A, and 5B in Cad11 (Fig. 6c), in a region on chromosome 2B in Cad12 (Fig. 6d), and in several regions of most chromosomes in environment Prn11 (Fig. 6e). Chromosome position (in cM) and the markers with the highest absolute value (in Mg ha^{-1}) for trait GY outlined in Fig. 6 are given in Supplemental Table S2 (see http://hdl.handle.net/11529/10233).

Table 3. Estimated posterior residual variance components (and their posterior standard deviations, SD) and the estimated posterior probability of markers with nonnull effects from the single-environment model BayesB model (sBB), the marker × environment interaction BayesB model (M×E BB), and the across-environment BayesB model (aBB) for four traits: grain yield (GY), grain volume weight (GVW), 1000-kernel weight (GWT), and days to heading (HD) measured in four environments (Arg12, Cad11, Cad12, and Pr11).

Component	Environment	GY		GVW		GWT		HD	
		Estimate	SD	Estimate	SD	Estimate	SD	Estimate	SD
		Single-environment BayesB (sBB)							
Residual	Arg12	0.7228	0.0703	0.7658	0.0734	0.3228	0.0354	0.4796	0.0492
	Cad11	0.8001	0.0715	0.9162	0.0754	0.3414	0.0369	0.3172	0.0352
	Cad12	0.8460	0.0743	0.5614	0.0619	0.4146	0.044	0.3952	0.0445
	Pr11	0.7759	0.0744	0.8834	0.0756	0.3336	0.0374	0.3784	0.0381
Probability	Arg12	0.4903	0.1518	0.5162	0.1483	0.4394	0.1663	0.1341	0.0491
	Cad11	0.4930	0.1406	0.5038	0.1472	0.4601	0.1676	0.1612	0.0619
	Cad12	0.5112	0.1407	0.5165	0.1425	0.4372	0.1655	0.1457	0.0546
	Pr11	0.5110	0.1476	0.4953	0.1509	0.4492	0.1723	0.1534	0.0579
		M × E interaction BayesB (M×E BB)							
Residual	Arg12	0.6314	0.0651	0.7138	0.0695	0.1255	0.0139	0.2247	0.0209
	Cad11	0.6827	0.0617	0.8994	0.0799	0.1787	0.018	0.0843	0.0095
	Cad12	0.7672	0.0771	0.5570	0.0642	0.2654	0.0279	0.1674	0.0184
	Pr11	0.6764	0.0604	0.8737	0.0727	0.1608	0.0161	0.1037	0.011
Probability	Main effect	0.5115	0.1182	0.5312	0.1134	0.4850	0.1089	0.4074	0.1215
	Arg12	0.4038	0.1094	0.4517	0.0979	0.2587	0.0959	0.3549	0.1377
	Cad11	0.5037	0.1056	0.5146	0.0913	0.5245	0.1012	0.4396	0.0861
	Cad12	0.5178	0.0929	0.4849	0.1045	0.4779	0.1117	0.4660	0.1183
	Pr11	0.5077	0.0958	0.5143	0.0937	0.5106	0.0904	0.4889	0.1067
		Across-environment BayesB (aBB)							
Residual	Arg12	0.7428	0.0666	0.7801	0.0698	0.1390	0.0140	0.2768	0.0250
	Cad11	0.7289	0.0636	1.0597	0.0911	0.2058	0.0195	0.1129	0.0124
	Cad12	1.0076	0.0838	0.7309	0.0662	0.3118	0.0267	0.2541	0.0227
	Pr11	0.7042	0.0644	0.9057	0.0784	0.1742	0.0173	0.1256	0.0134
Probability	All	0.3935	0.1237	0.3482	0.0959	0.2857	0.0886	0.1334	0.0385

Prediction Accuracy of the Single-Environment and Marker × Environment Interaction Bayesian Ridge Regression and the BayesB Models

For this section, analyses using 50 random cross-validation partitions of the data in TRN and TST sets were performed with the aim of assessing prediction accuracy of the various models. Prediction accuracies of the single-environment, M×E, and across-environments models derived from models BRR and BB in each of the four environments for two traits, GY and HD, in the two cross-validation schemes, CV1 and CV2, are shown in Figs. 7a–b (GY) and Figs. 7c–d (HD).

For GY, all correlations in CV1 (Fig. 7a) are lower (<0.3) than in CV2 (Fig. 7b) (<0.45) for all environments and models. In CV2, models M×E BB, M×E BRR, aBB, and aBRR had higher prediction accuracy than the single-environment (sBB and sBRR) in all environments, except for Cad12 (Fig. 7b). Also, for GY in CV2, prediction accuracy of M×E BB was higher than that of M×E BRR in all environments except Cad12, which had a correlation for CV2 similar to those achieved in CV1. The smallest correlations were obtained by sBB and sBRR models for CV1 and CV2 in all environments, except environment Cad12, which showed the smallest correlations for all models, especially for aBB and aBRR in CV1 and CV2. Prediction accuracy patterns for GY in CV1 (Fig. 7a) show models M×E BB and BB with similar accuracies in all four environments and slightly superior to other models in all the environments. Supplemental Table S3 (see http://hdl.handle.net/11529/10233) shows the correlations between observed and predicted values for M×E, single-environment, and across-environment models derived from BB and BRR models for cross-validations CV1 and CV2 for all traits in all environments.

For trait HD, all predictions in CV1 (Fig. 7c) (<0.75) are lower than in CV2 (Fig. 7d) (<0.95) for all environments and models. However, general prediction accuracy patterns are clearer in HD than in GY. For CV1, the best predicted model was sBB, followed by M×E BB and aBB. For CV1, models aBRR and sBRR were consistently the worst for all traits and environments. In general, prediction accuracies of BB were always better than BRR, reaching predictions of up to 0.7 for CV1. For CV2 (Fig. 7d), the best

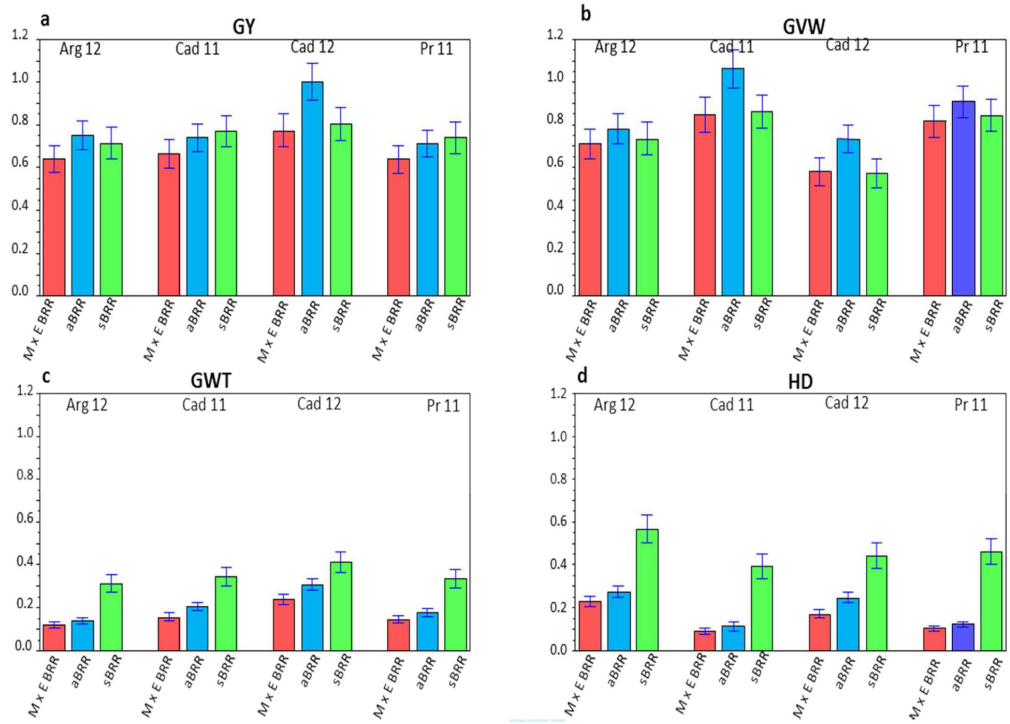

Figure 2. Histograms of the residual variance components and their error bars (standard deviation) of three models: marker × environment interaction Bayesian ridge regression (M×E BRR), across-environment Bayesian ridge regression (aBRR), and single-environment Bayesian ridge regression (sBRR) for four traits, (a) grain yield (GY), (b) grain volume weight (GVW), (c) 1000-kernel weight (GWT), and (d) days to heading (HD) evaluated in four environments (Arg12, Cad11, Cad12, and Pr11).

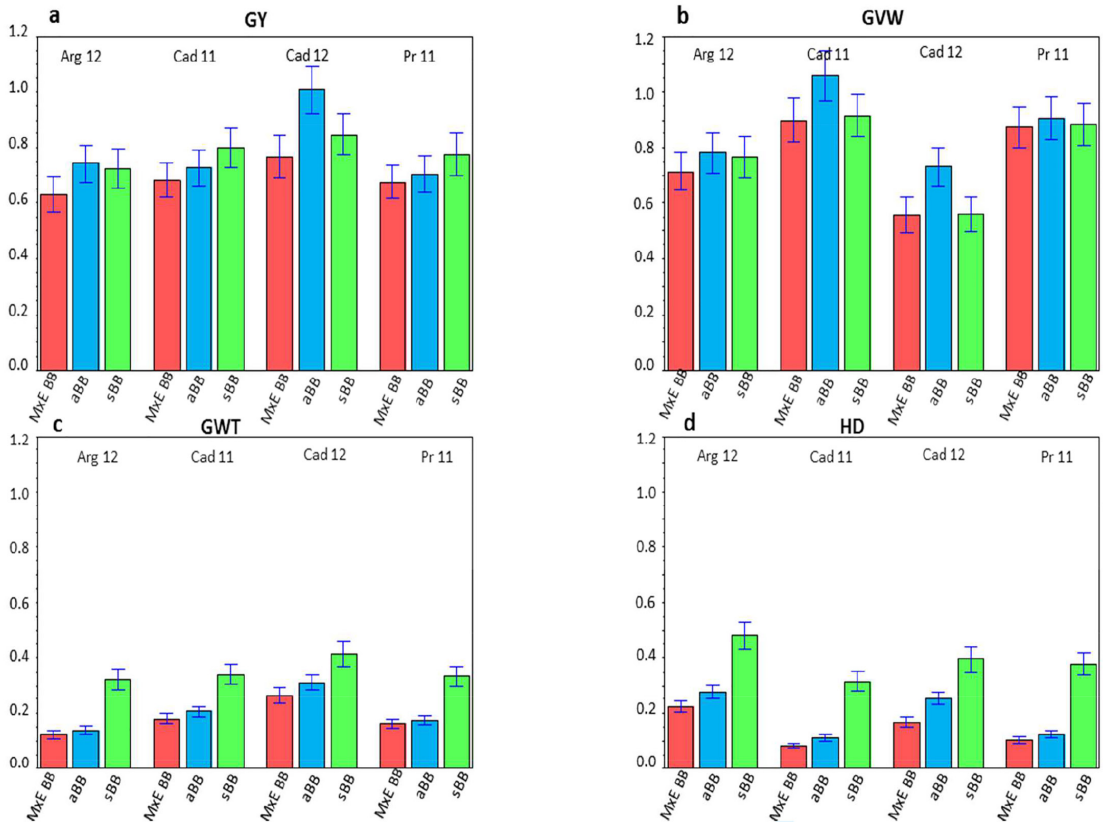

Figure 3. Histograms of the residual variance components and their error bars (standard deviation) of three models: marker × environment interaction BayesB (M×E BB), across-environment BayesB (aBB), and single-environment BayesB (sBB) for four traits (a) grain yield (GY), (b) grain volume weight (GVW), (c) 1000-kernel weight (GWT), and (d) days to heading (HD) evaluated in four environments (Arg12, Cad11, Cad12, and Pr11).

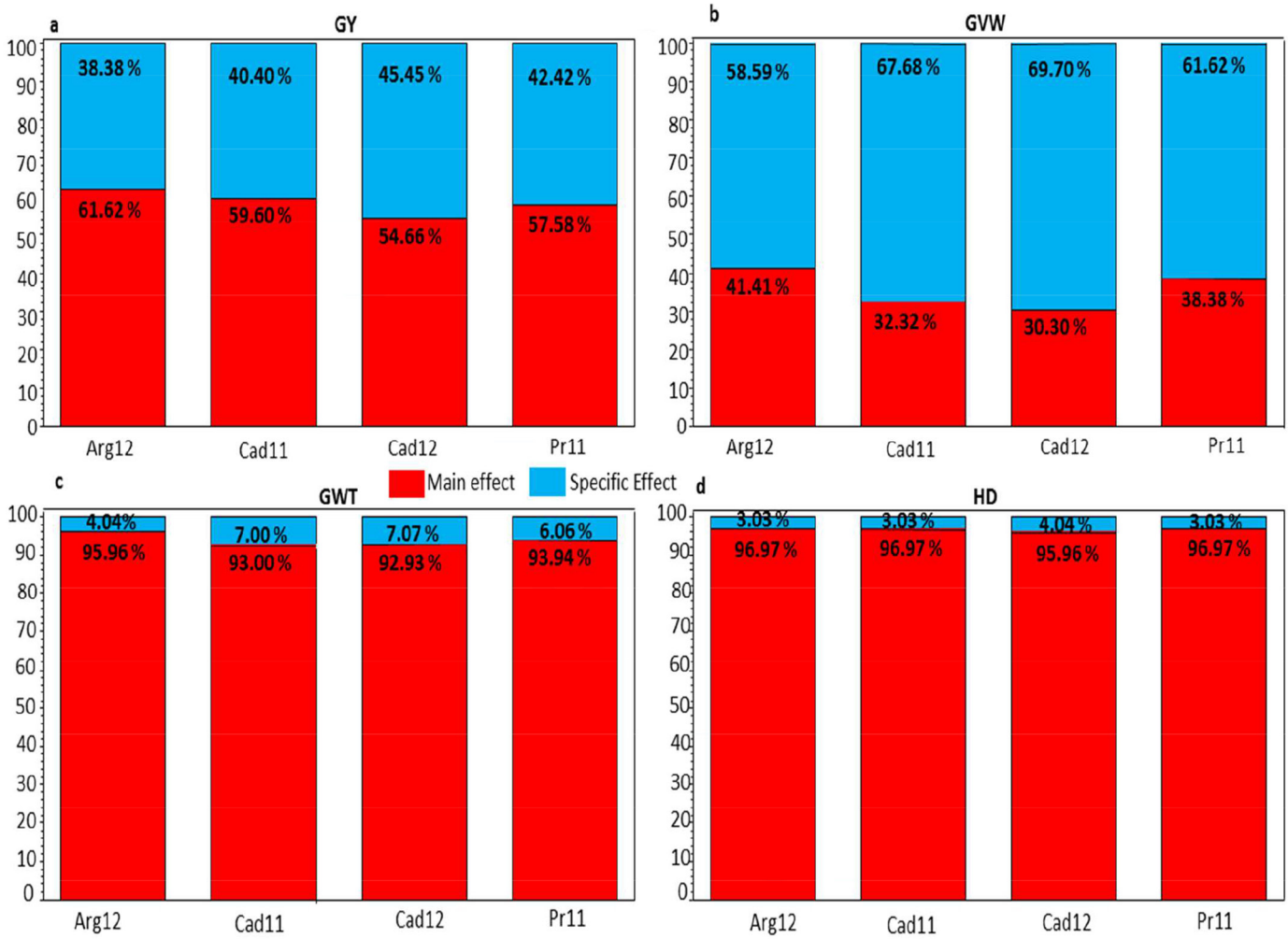

Figure 4. Bar plot of the percentage of the total genomic variance explained by the marker main effect (red) and the environment-specific effect (blue) variance components from the marker × environment interaction Bayesian ridge regression model (BRR) for four traits: (a) grain yield (GY), (b) grain volume weight (GVW), (c) 1000-kernel weight (GWT), and (d) days to heading (HD) evaluated in four environments (Arg12, Cad11, Cad12, and Pr11).

predictive model for all traits and environments was M×E BB, closely followed by M×E BRR, aBB and aBRR, reaching predictions of up to 0.93. The worst models for CV2 were always sBRR and sBB. In summary, results show high correlations between observed and predicted values for HD and intermediate-to-low prediction accuracies for GY. Prediction accuracies for traits GVW and GWT are depicted in Supplemental Figs. S1a–b (GVW) and Supplemental Figs. S2a–b (GWT), respectively (see http://hdl.handle.net/11529/10233). Trait GVW shows intermediate-to-low patterns of prediction accuracy similar to GY, and trait GWT shows high prediction accuracies similar to trait HD.

Results in terms of average prediction accuracy over environments are reported in Table 4. For CV1, the M×E BB and BRR models had better prediction accuracy than the single- and across-environment BB and BRR models for traits GY and GVW and similar accuracy to the across-environment BB and BRR models for traits HD and GWT. However, for BB-HD and BRR-GWT, the single-environment model was better than the other models. In contrast, for CV2, the average superiority in terms of prediction accuracy of the M×E BB and BRR models over the other two models is clear for all traits. Note that the prediction accuracy of sBRR and sBB models was low for HD and GWT (CV2). For CV2, prediction accuracy of the M×E BB model was higher than those of the sBB and aBB models, which had correlations ranging from 0.2657 for GVW to 0.8753 for GWT compared with correlations of 0.2300 for GVW and 0.6934 for GWT for the sBB model (Table 4).

Another way to represent the prediction accuracy patterns of the different models is to plot the correlations from the M×E model on the vertical axis vs. correlations from the single-environment model on the horizontal axis, and then the M×E model on the vertical axis vs. the across-environment model on the horizontal axis (Fig. 8). The model–trait combinations above the 45° line represent the average correlations of the method whose predictive correlation is given on the vertical axis.

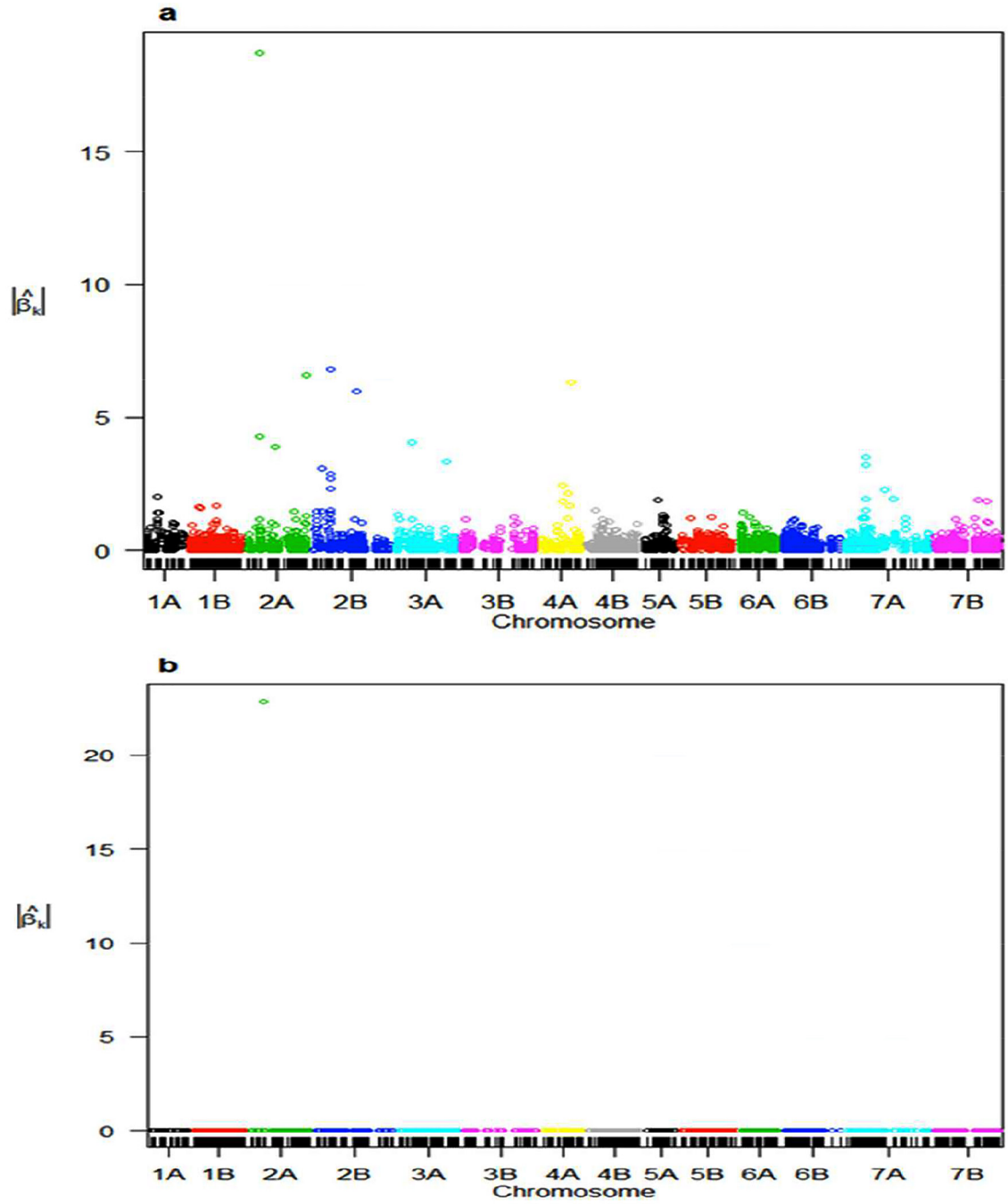

Figure 5. Absolute value of the estimated marker effects (*y*-axis) ($|\hat{\beta}_k|$) or heading days (HD) vs. chromosome marker position (*x*-axis) obtained from the marker × environment interaction BayesB (BB) model for the full data. (a) Marker main effect; (b) effect specific to environment Cad11.

The M×E model outperformed the model whose correlation is given on the horizontal axis for the CV1 and CV2 cross-validation schemes. As previously described for CV1, the prediction accuracy of the M×E model was very similar to that of the single-environment (except for BB-GWT, BRR-GWT, and BB-HD that were slightly better for the single-environment model than for the M×E model) and across-environment models (Fig. 8a,b). For CV2, the M×E model had better accuracy than the single-environment model (Fig. 8c) and was similar to the across-environment model. Finally, Supplemental Fig. S3a–f (see http://hdl.handle.net/11529/10233) depict, in a horizontal box plot, the average prediction accuracy over environments for CV1 and CV2 and all four traits for the M×E BB and BRR models (Supplemental Fig. S3a d), sBB and BRR models (Supplemental Fig. S3c, f), and aBB and BRR models (Supplemental Fig. S3b, e).

DISCUSSION

The durum wheat population used in this study is a balanced NCCR population that shows null or negligible population structure effects (Milner et al., 2015), that is, the

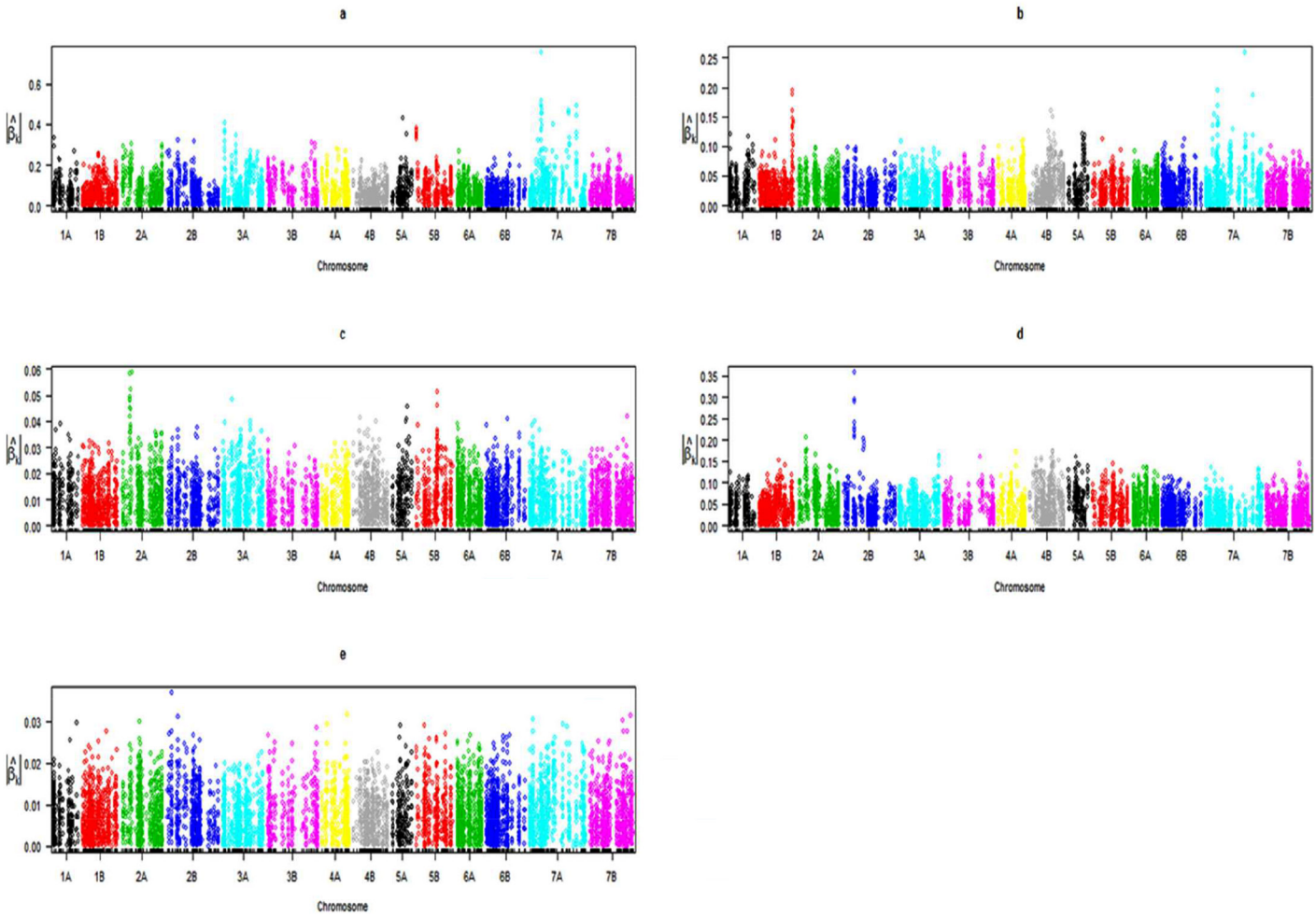

Figure 6. Absolute value of the estimated marker effects (*y*-axis) ($|\hat{\beta}_k|$) for grain yield (GY) vs. chromosome marker position (*x*-axis) obtained from the marker × environment interaction BayesB (BB) model for the full data. (a) Marker main effect; (b) marker effect specific to environment Arg 12; (c) marker effect specific to environment Cad11; (d) marker effect specific to environment Cad12; (e) marker effect specific to environment Prn11.

nonrandom assortment of genetic backgrounds in individuals of the target population, a factor that strongly affects the correct inference of genetic and marker effects on phenotype. Therefore, the NCCR population provides a more suitable material for assessing the performance of M×E models than the collections of diverse cultivars and breeding lines commonly used in association mapping studies.

In this study, we extended the original model of López-Cruz et al. (2015), which assumes homogeneous error variance across environments, to a model that accommodates environment-specific variances. Another difference with respect to the López-Cruz et al. (2015) model is that we used a prior that induces differential shrinkage of estimates and variable selection (de los Campos et al., 2013); this allows achieving good prediction accuracy while identifying sets of markers with effects that are stable across environments and others that are responsible for M×E and thus genotype × environment interaction.

The Association of Marker Main Effects and Environment-Specific Effects of the Marker × Environment Interaction Models in Durum Wheat Traits

In this study, we show that the M×E derived from the BayesB model can have the dual purpose of predicting the genomic performance of untested durum wheat lines in certain environments and assessing the association of chromosome regions with (i) marker main effects across environments and (ii) markers in chromosome regions that are affected by specific environmental conditions (M×E). The prior distribution assigned to BB induces marker shrinkage as well as marker selection.

For example, we found that regions of chromosomes 2A, 2B, and 7A had important marker main effects for HD. These regions coincided with those harboring major photoperiod and phenology regulators such as loci *PPD* and *FT*, as reported by Milner et al. (2015). Notably, the M×E model was able to point out specific marker effects in environments such as the effect in chromosome 2A (*PPD-A1*)

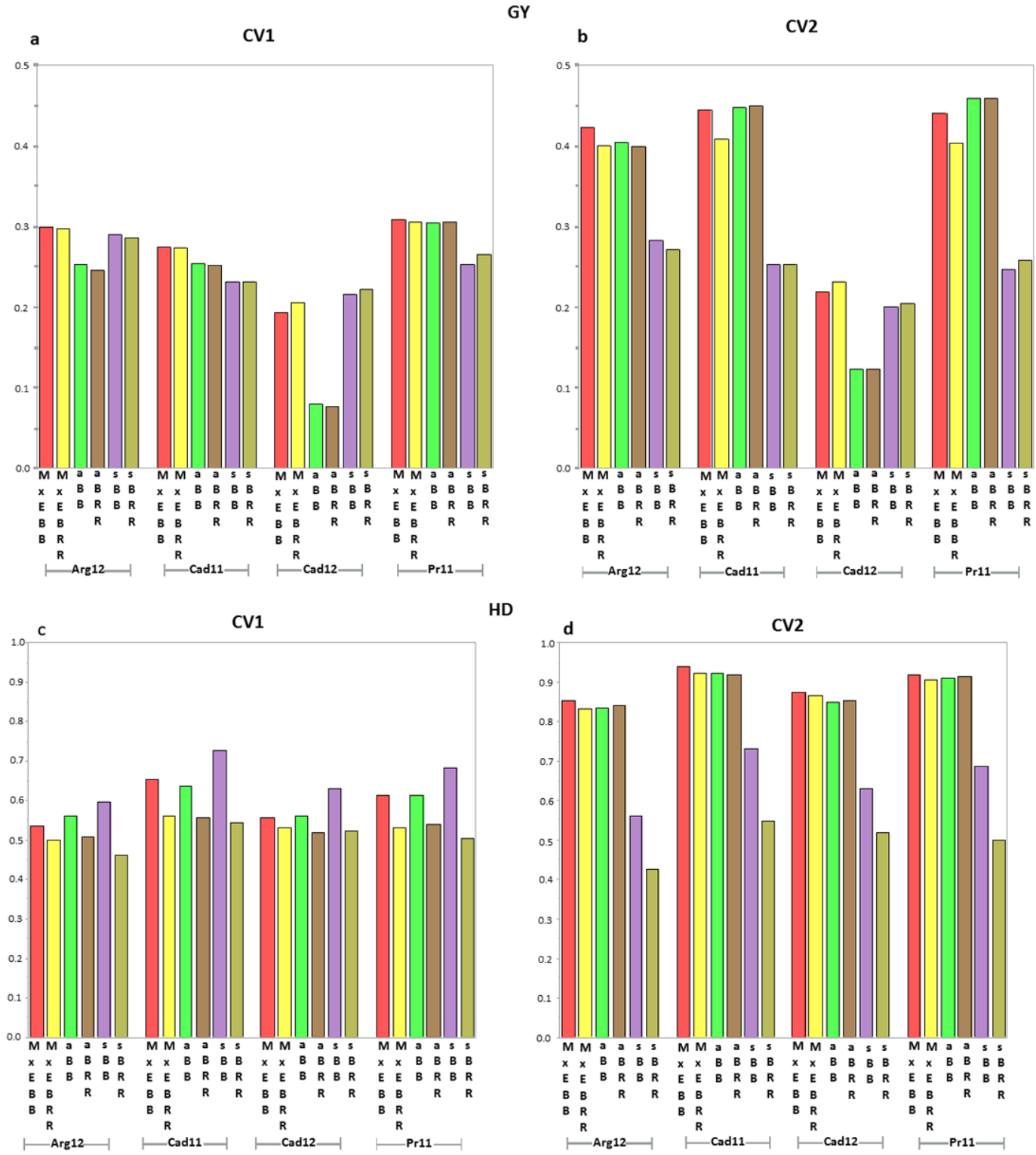

Figure 7. Histograms of the average correlations (50 training–testing partitions) for grain yield (GY) in each of the four environments (Arg12, Cad11, Cad12, and Pr11) of models marker (M) × environment (E) interaction Bayesian ridge regression (M×E BRR), M × E interaction BayesB (M×E BB), single-environment Bayesian ridge regression (sBRR), single-environment BayesB (sBB), across-environment Bayesian ridge regression (aBRR), and across-environment BayesB (aBB) for (a) cross-validation CV1 and (b) cross-validation CV2. For trait days to heading (HD) (c) cross-validation CV1, and (d) cross-validation CV2.

that is favored in environment Cad11 and those markers in chromosomes 2A and 2B (*PPD-A1* and *PPD-B1*) that are favored in Prn11 as well as the specific effect of chromosome 7A (*TaFT-A*) in Cad12. Interestingly, in addition to the strong and specific effects of chromosomes 2 and 7, the model revealed effects at chromosomes 3A, 4A, 4B, 5A, and 5B, which have been shown to carry minor QTLs for HD in wheat, including durum wheat (Maccaferri et al., 2014).

Table 4. Mean correlation between observed and predicted values and their standard deviation (SD) across 50 training–testing set partitions from the marker (M) × environment (E) interaction, single-environment, and across-environment Bayesian ridge regression (BRR) and BayesB (BB) models for four traits: grain yield (GY), grain volume weight (GVW), 1000-kernel weight (GWT), and days to heading (HD) across four environments for two cross-validation schemes (CV1 and CV2).

	BRR-GY	BB-GY	BRR-GVW	BB-GVW	BRR-HD	BB-HD	BRR-GWT	BB-GWT
	Cross-validation scheme CV1							
M × E interaction	0.2710	0.2692	0.2447	0.2428	0.5310	0.5880	0.6431	0.6746
SD	0.0741	0.0734	0.0492	0.0475	0.0781	0.0646	0.0522	0.0499
Across environment	0.2204	0.2231	0.2050	0.2054	0.5306	0.5922	0.6440	0.6764
SD	0.0829	0.0825	0.0535	0.0528	0.0768	0.0661	0.0534	0.0490
Single environment	0.2515	0.2483	0.2414	0.2462	0.5074	0.6597	0.6646	0.6986
SD	0.0664	0.0650	0.0484	0.0484	0.0791	0.0547	0.0507	0.0452
	Cross-validation scheme CV2							
M × E interaction	0.3600	0.3813	0.2600	0.2657	0.8815	0.8970	0.8702	0.8753
SD	0.0444	0.0448	0.0452	0.0461	0.0206	0.0189	0.0097	0.0095
Across environment	0.3571	0.3586	0.2592	0.2591	0.8817	0.8796	0.8721	0.8718
SD	0.0417	0.0423	0.0451	0.0451	0.0198	0.0198	0.0096	0.0099
Single environment	0.2455	0.2452	0.2254	0.2300	0.4968	0.6528	0.6611	0.6934
SD	0.0534	0.0530	0.0470	0.0478	0.0289	0.0238	0.0234	0.0216

Detecting regions for a complex trait such as GY is more complicated because many more loci are involved in the expression of the trait, and M×E patterns are consequently more complex. Nevertheless, the M×E BB model detected marker main effects in regions of chromosomes 2B and 7A, again involving *PPD-A1* and *TaFT-A1*, which also had important environment-specific GY marker effects in environments Arg12, Cad12, and Prn11. These two chromosome regions were detected as important by Milner et al. (2015) in their QTL study. However, as compared with a standard QTL analysis (Milner et al., 2015), the models used in this approach were more efficient in identifying overall and environment-specific additional marker effects associated with GY.

Variance Components on Residual and Marker Main and Specific Effects

In general, results of this study agreed with those found by López-Cruz et al. (2015), where the M×E model fitted the data better than the across-environment and single-environment models. It is also clear that the estimates of variance components from the M×E model indicated that the proportion of genomic variance explained by the main effect of markers is directly related to the (empirical sample) phenotypic correlation between environments. In this study, traits HD and GWT had positive and high sample phenotypic correlations among environments, whereas traits GY and GVW had small and close-to-zero correlations among several pairs of environments.

The across-environment models had relatively higher residual variance than the M×E model, indicating that forcing constant marker effects across the environments, $\mathbf{b}_1 = \mathbf{b}_2 = \cdots = \mathbf{b}_s = \mathbf{b}$, does not produce a better fit of this model. The residuals of the M×E BRR model tended to be more similar to those of the sBRR model, especially for traits GY and GVW (Fig. 2a, b). However, for traits GWT and HD, the opposite occurred, that is, residuals from the M×E model and the across-environment models were more similar and smaller than those from the single-environment model, which showed large residual variances (Fig. 2c, d). Similar trends are found for the residuals of the BB model. Models fit the data better for less complex traits, HD and GWT, than the data from more complex traits such as GY and GVW.

Also, variance components resulting from marker main effects are much smaller in less complex traits (HD and GWT) than in GY and GVW. The opposite occurred for variance components of specific marker effects (in environments), where complex traits like GY and GVW show higher M×E than HD and GWT.

Prediction Accuracy of the Marker × Environment Model

The study of López-Cruz et al. (2015) in bread wheat demonstrated that for cross-validation 2 (CV2), the M×E model always showed higher prediction accuracy than the across-environment model, and higher than or the same prediction accuracy as the single-environment model. The M×E model is based on variance component estimation of the marker main effects and environment-specific marker effects and, in terms of prediction accuracy, it performed well in positively correlated environments. Based on this assumption, the M×E model will tend to have higher prediction accuracy for traits that have positive correlations between environments (HD and GWT) than for traits that have close to zero or negative correlations between environments (GY and GVW) (Table 1).

In the M×E model, the marker effect has two components: one is a result of overall marker effects across environments and the other one resulting from marker effects

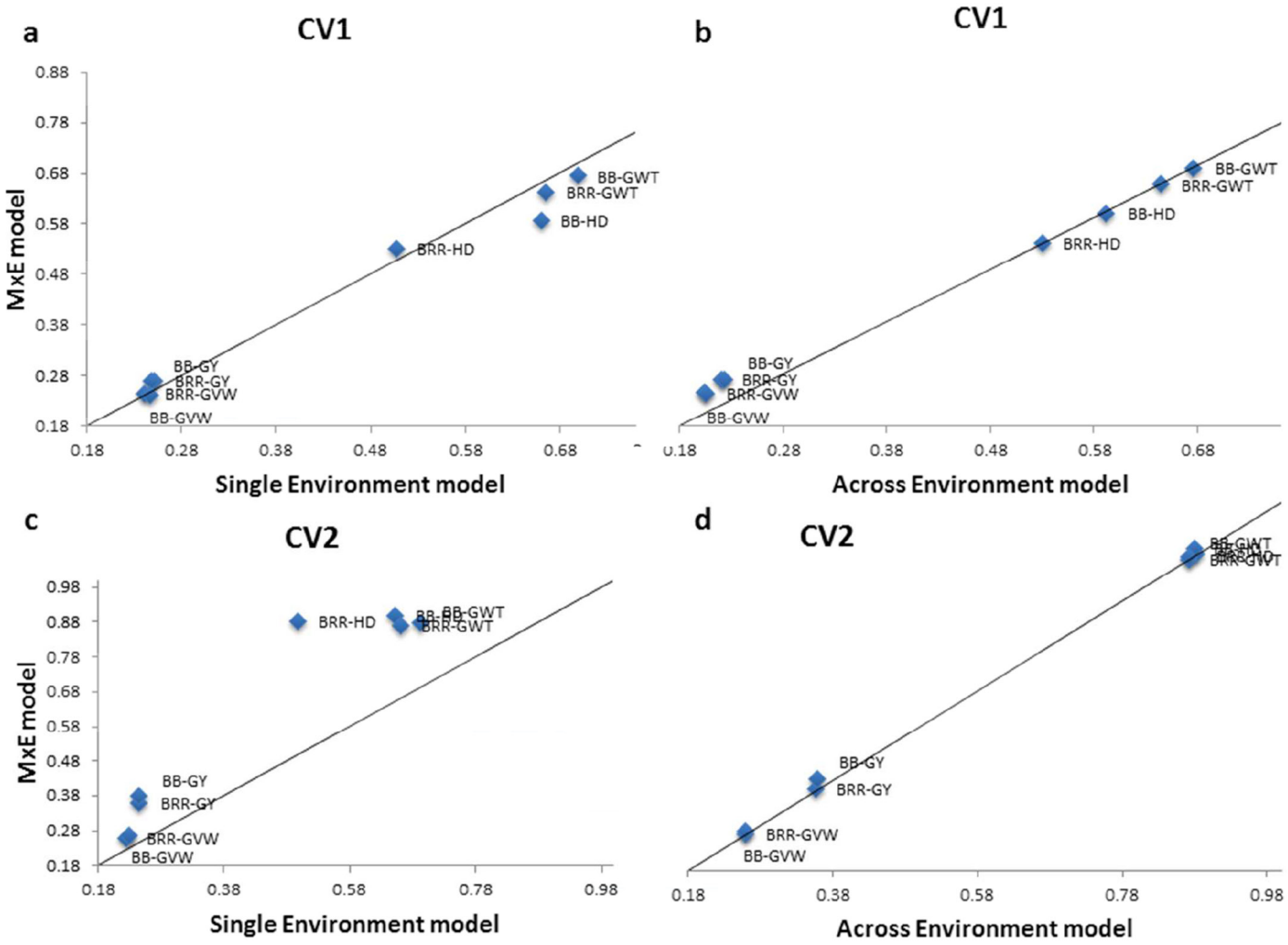

Figure 8. Plot of the average correlation (50 training–testing partitions) across four environments of the (a) marker (M) × environment (E) interaction Bayesian ridge regression (BRR) and Bayesian BayesB (BB) models vs. the single-environment BRR and BB models, and the (b) M × E interaction BRR and BBmodels vs. the across-environment BRR and BB models for four traits, grain yield (GY), grain volume weight (GVW), 1000-kernel weight (GWT), and heading days (HD), and for cross-validation CV1. For cross-validation CV2, (c) M × E interaction BRR and BB models vs. the single-environment BRR and BB models and the (d) M × E interaction BRR and BB models vs. the across-environment BRR and BB models for four traits: GY, GVW, GWT, and HD. The solid line represents $Y = X$, that is, both models have the same prediction ability. The prediction accuracy of the best models (above the solid line), M × E interaction BRR and BB, are shown. The superior predictions of the single-environment or across-environment BRR and BB are shown below the line.

in specific environments. When the proportion of variance explained by the marker main effect is relatively high (such as in traits HD and GWT) (Table 2; Fig. 4c,d), the number of effective markers with nonnull effects should be relatively small (Table 3). The M×E is not complex and this is reflected in both traits having high heritability; therefore, the M×E model has relatively high prediction accuracy in most environments (Table 4).

On the other hand, when the proportion of variance explained by the marker main effect is small (<3%) and the relative contribution of the specific marker effect is higher than that of the main effect, such as in GVW (Table 2), the M×E is complex and therefore the number of effective markers with nonnull effect in some environments will be large (Table 3). This is reflected in the trait having low heritability; the M×E model therefore has intermediate-to-low prediction accuracy in most environments. An intermediate case is trait GY, which has relatively high marker main effects as well as specific effects, and a relatively high proportion of markers with nonnull effect in many environments.

In this study, we show that the M×E model is flexible and can be used with different priors commonly used in genomic selection. In the durum wheat study reported herein, we used the M×E model with (i) the Gaussian prior of the BRR (or GBLUP) that induces shrinkage and (ii) a prior that combines properties of the M×E model (separates marker effects into main and environment-specific effects), while inducing variable selection, such as the BB model that has peak mass at zero with the marker

effects assumed to be equal to zero with probability π and assumed to be a draw from a *t*-distribution with probability (1 − π). This flexibility of the M×E model allows mapping stable casual loci across environments and identifying loci that are favored by specific environments, that is, mapping specific positive interactions between chromosome regions and environments. For this data set, the BB model seems to accomplish both tasks, that is, it gives good prediction accuracy while identifying regions of chromosomes with important effects on phenotypic traits.

The effects of some markers are often known in advance. For example, in our study, major players for phenology were known; thus, it was possible to include their markers in the regression models and modify the prior specification such that with a probability of one, these markers were included in the model. Further research is needed to add this feature to the M×E BB and BRR models.

CONCLUSIONS

In this study targeting durum wheat as a cereal crop, we used an M×E model that allows (i) assessing the genomic prediction accuracy for several traits having different degrees of genetic complexity and (ii) identifying chromosome regions associated with stable phenotypic effects across environments, as well as specific chromosome regions that harbor loci providing adaptation to specific environments. The interaction model used a Gaussian prior (BRR) or a BB prior. In terms of minimizing the model residual variance, the M×E model outperformed the more traditional single-environment and across-environment models. Traits HD and GWT, whose genetic control is based on well-identified loci with large effects, showed a relatively higher overall variance component of marker effect and a smaller environment-specific variance component than more complex traits such as GY and GVW. Additionally, HD and GWT had higher prediction accuracy than GY and GVW, as expected. In general, of the two tested prior models, the BB model gave higher prediction accuracy than the BRR model for most model-trait combinations. For cross-validation problem CV2, the M×E model derived from BRR or BB had better prediction accuracy than the single-environment or across-environment models. As expected, results of prediction accuracy for CV1 were not as clear as for CV2 and the M×E model was not always the best predictive model for all traits.

Regarding the identification of chromosome regions with stable effects across environments and those with effects specific to an environment, the M×E model clearly identified the presence of both types of effects in regions of chromosomes 2A, 2B, 7A associated with the well-known *PPD* and *FT* loci. Additional regions with mainly environment-specific signals were uncovered in chromosome groups 3, 4, and 5, known to harbor QTLs for HD in wheat. For a very complex trait such as GY, in addition to the side effects of *PPD* and *FT* loci, other chromosome regions with appreciable marker effects were detected in chromosome groups 1, 2, 3, 4, 5, and 7. Notably, markers in chromosomes 5A and 5B showed stable effects across environments and also in specific environments (Arg12 and Prn11).

References

Abdalla, O.S., J. Crossa, and P.L. Cornelius. 1997. Results and biological interpretation of shifted multiplicative model clustering of durum wheat cultivars and test site. Crop Sci. 37:88–97. doi:10.2135/cropsci1997.0011183X003700010014x

Bennett, D., M. Reynolds, D. Mullan, A. Izanloo, H. Kuchel, P. Langridge, and T. Schnurbusch. 2012. Detection of two major grain yield QTL in bread wheat (*Triticum aestivum* L.) under heat, drought and high yield potential environments. Theor. Appl. Genet. 125:1473–1485. doi:10.1007/s00122-012-1927-2

Bernardo, R., and J. Yu. 2007. Prospects for genome-wide selection for quantitative traits in maize. Crop Sci. 47:1082–1090. doi:10.2135/cropsci2006.11.0690

Beyene, Y., K. Semagn, S. Mugo, A. Tarekegne, R. Babu, B. Meisel, P. Sehabiague, D. Makumbi, C. Magorokosho, S. Oikeh, J. Gakunga, M. Vargas, M. Olsen, B. M. Prasanna, M. Banziger, and J. Crossa. 2015. Genetic gains in grain yield through genomic selection in eight bi-parental maize populations under drought stress. Crop Sci. 55:154–163. doi:10.2135/cropsci2014.07.0460

Boer, M.P., D. Wright, L. Feng, D.W. Podlich, L. Luo, et al. 2007. A mixed-model quantitative trait loci (QTL) analysis for multiple-environment trial data using environmental covariables for QTL-by-environment interactions, with an example in maize. Genetics 177:1801–1813. doi:10.1534/genetics.107.071068

Bonneau, J., J. Taylor, B. Parent, D. Bennett, M. Reynolds, C. Feuillet, P. Langridge, and D. Mather. 2013. Multi-environment analysis and improved mapping of a yield-related QTL on chromosome 3B of wheat. Theor. Appl. Genet. 126:747–761. doi:10.1007/s00122-012-2015-3

Burgueño, J., J. Crossa, P.L. Cornelius, R. Trethowan, G. McLaren, and A. Krishnamachari. 2007. Modeling additive × environment and additive × additive × environment using genetic covariance of relatives of wheat genotypes. Crop Sci. 47:311–320. doi:10.2135/cropsci2006.09.0564

Burgueño, J., G. de los Campos, K. Weigel, and J. Crossa. 2012. Genomic prediction of breeding values when modeling genotype × environment interaction using pedigree and dense molecular markers. Crop Sci. 52:707–719. doi:10.2135/cropsci2011.06.0299

Cockerham, C.C. 1963. Estimation of genetic variances. In: W.D. Hanson and H.F. Robinson, editors, Statistical genetics and plant breeding. National Academy of Sciences–National Research Council Publication 982, Washington, DC. p. 53–93.

Collins, N.C., F. Tardieu, and R. Tuberosa. 2008. QTL approaches for improving crop performance under abiotic stress conditions: Where do we stand? Plant Physiol. 147:469–486. doi:10.1104/pp.108.118117

Cornelius, P.L., J. Crossa, and M.S. Seyedsadr. 1996. Statistical tests and estimators of multiplicative models for genotype-by-environment interaction. In: M.S. Kang and H.G. Gauch, editors, Genotype-by-environment interaction. CRC Press, Boca Raton, FL. p. 199–234.

Crossa, J., J. Burgueño, P.L. Cornelius, R. Trethowan, and A. Krishnamachari. 2006. Modeling genotype × environment interaction using additive genetic covariances of relatives for predicting breeding values of wheat genotypes. Crop Sci. 46:1722–1733. doi:10.2135/cropsci2005.11-0427

Crossa, J., G. de los Campos, P. Pérez-Rodríguez, D. Gianola, J. Burgueño, et al. 2010. Prediction of genetic values of quantitative traits in plant breeding using pedigree and molecular markers. Genetics 186:713–724. doi:10.1534/genetics.110.118521

de los Campos, G., D. Gianola, G.J.M. Rosa, K. Weigel, and J. Crossa. 2010. Semi-parametric genomic-enabled prediction of genetic values using reproducing kernel Hilbert spaces methods. Genet. Res. 92:295–308. doi:10.1017/S0016672310000285

de los Campos, G., J.M. Hickey, R. Pong-Wong, H.D. Daetwyler, and M.P.L. Calus. 2013. Whole-genome regression and prediction methods applied to plant and animal breeding. Genetics 193:327–345. doi:10.1534/genetics.112.143313

de los Campos, G., H. Naya, D. Gianola, J. Crossa, A. Legarra, et al. 2009. Predicting quantitative traits with regression models for dense molecular markers and pedigree. Genetics 182:375–385. doi:10.1534/genetics.109.101501

de los Campos, G., and P. Pérez-Rodríguez. 2015. Bayesian generalized linear regression. R package version 1.0.4. CRAN. https://cran.r-project.org/web/packages/BGLR/index.html (accessed 03 Nov. 2015).

Dickerson, G.E. 1962. Implications of genetic environmental interaction in animal breeding. Animal Production 4:47–63. doi:10.1017/S0003356100034395

El-Soda, M., W. Kruijer, M. Malosetti, M. Koornneef, and M.G. Aarts. 2014. Quantitative trait loci and candidate genes underlying genotype by environment interaction in the response of *Arabidopsis thaliana* to drought. Plant Cell Environ. 38:585–599. doi:10.1111/pce.12418

Falconer, D.S. 1952. The problem of environment and selection. Am. Nat. 86:293–298. doi:10.1086/281736

Gianola, D. 2013. Priors in whole-genome regression: The Bayesian alphabet returns. Genetics 90:525–540. doi:10.1017/S0016672308009890

González-Camacho, J.M., G. de los Campos, P. Pérez-Rodríguez, D. Gianola, et al. 2012. Genome-enabled prediction of genetic values using radial basis function. Theor. Appl. Genet. 125:759–771. doi:10.1007/s00122-012-1868-9

Heslot, N., D. Akdemir, M.E. Sorrells, and J.L. Jannink. 2014. Integrating environmental covariates and crop modeling into the genomic selection framework to predict genotype by environment interactions. Theor. Appl. Genet. 127:463–480. doi:10.1007/s00122-013-2231-5

Heslot, N., H.P. Yang, M.E. Sorrells, and J.L. Jannink. 2012. Genomic selection in plant breeding: A comparison of models. Crop Sci. 52:146–160. doi:10.2135/cropsci2011.06.0297

Huang, B.E., and A.W. George. 2011. R/mpMap: A computational platform for the genetic analysis of multiparent recombinant inbred lines. Bioinformatics 27:727–729. doi:10.1093/bioinformatics/btq719

Jarquín, D., J. Crossa, X. Lacaze, P.D. Cheyron, J. Daucourt, et al. 2014. A reaction norm model for genomic selection using high-dimensional genomic and environmental data. Theor. Appl. Genet. 127:595–607. doi:10.1007/s00122-013-2243-1

López-Cruz, M., J. Crossa, D. Bonnett, S. Dreisigacker, J. Poland, J-L. Jannink, R.P. Singh, E. Autrique, and G. de los Campos. 2015. Increased prediction accuracy in wheat breeding trials using a marker × environment interaction genomic selection model. G3: Genes, Genomes, Genet. 5:569–582. doi:10.1534/g3.114.016097

Maccaferri, M., A. Ricci, S. Salvi, S.G. Milner, E. Noli, P.L. Martelli, R. Casadio, E. Akhunov, K. Ammar, A. Blanco, F. Desiderio, A. Distelfeld, J. Dubcovsky, T. Fahima, J. Faris, A. Korol, A. Massi, A. Mastrangelo, M. Morgante, C. Pozniak, S. Xu, and R. Tuberosa. 2014. A high-density SNP based map of tetraploid wheat. Plant Biotechnol. J. 13:648–663. doi:10.1111/pbi.12288

Maccaferri, M., M.C. Sanguineti, S. Corneti, J.L.A. Ortega, M. Ben Salem, J. Bort, E. DeAmbrogio, L.F.G. Del Moral, A. Demontis, A. El-Ahmed, F. Maalouf, H. Machlab, V. Martos, M. Moragues, I. Motawaj, M. Nachit, N. Nserallah, H. Ouabbou, C. Royo, A. Slama, and R. Tuberosa. 2008. Quantitative trait loci for grain yield and adaptation of durum wheat (*Triticum durum* Desf.) across a wide range of water availability. Genetics 178:489–511. doi:10.1534/genetics.107.077297

Maccaferri, M., M.C. Sanguineti, A. Demontis, A. El-Ahmed, L. Garcia Del Moral, F. Maalouf, M. Nachit, N. Nserallah, H. Ouabbou, S. Rhouma, C. Royo, D. Villegas, and R. Tuberosa. 2011. Association mapping in durum wheat grown across a broad range of water regimes. J. Exp. Bot. 62:409–438. doi:10.1093/jxb/erq287

Massman, J.M., H.J.G. Jung, and R. Bernardo. 2013. Genome-wide selection versus marker assisted recurrent selection to improve grain yield and stover-quality traits cellulosic ethanol in maize. Crop Sci. 53:58–66. doi:10.2135/cropsci2012.02.0112

Meuwissen, T.H.E., B.J. Hayes, and M.E. Goddard. 2001. Prediction of total genetic value using genome-wide dense marker maps. Genetics 157:1819–1829.

Milner, S.G., J. Maccaferri, B.E. Huang, P. Mantovani, A. Massi, E. Frascaroli, R. Tuberosa, and S. Salvi. 2015. A multiparental cross population for mapping QTLs for agronomic traits in durum wheat (*Triticum turgidum* ssp. *durum*). Plant Biotechnol. J. (online) doi:10.1111/pbi.12424

Moreau, L., A. Charcosset, and A. Gallais. 2004. Use of trial clustering to study QTL × environment effects for grain yield and related traits in maize. Theor. Appl. Genet. 110:92–105. doi:10.1007/s00122-004-1781-y

Pérez-Rodríguez, P., and G. de los Campos. 2014. Genome-wide regression and prediction with the BGLR statistical package. Genetics 198:483–495. doi:10.1534/genetics.114.164442

Pérez-Rodríguez, P., D. Gianola, J.M. González-Camacho, J. Crossa, Y. Manes, and S. Dreisigacker. 2012. Comparison between linear and non-parametric models for genome-enabled prediction in wheat. G3: Genes, Genomes, Genet. 2:1595–1605.

Piepho, H.P. 1997. Analyzing genotype–environment data by mixed models with multiplicative effects. Biometrics 53:761–766. doi:10.2307/2533976

Piepho, H.P. 1998. Empirical best linear unbiased prediction in cultivar trials using factor analytic variance-covariance structure. Theor. Appl. Genet. 97:195–201. doi:10.1007/s001220050885

R Development Core Team. 2014. R: A language and environment for statistical computing. R Foundation for Statistical Computing, Vienna, Austria. http://www.R-project.org/

Smith, A.B., B.R. Cullis, and R. Thompson. 2005. The analysis of crop cultivar breeding and evaluation trials: An overview of current mixed model approaches. J. Agric. Sci. 143:449–462. doi:10.1017/S0021859605005587

Trethowan, R.M., J. Crossa, and W.H. Pfeiffer. 2005. Management of genotype × environment interactions and their implications for durum wheat. In: C. Royo, M.M. Nachit, N. Di Fonzo, J.L. Araus, W.H. Pfeiffer, and G.A. Slafer, editors, Durum wheat breeding. Current approaches and future strategies. Vol. 2. The Haworth Press, New York. p. 777–801.